e-Prime - Advances in Electrical Engineering, Electronics and Energy 4 (2023) 100144

Contents lists available at ScienceDirect

e-Prime - Advances in Electrical Engineering, Electronics and Energy

journal homepage: www.elsevier.com/locate/prime

Reinforcement learning-based allocation of fog nodes for cloud-based smart grid

Muhammad Ali Jamshed [a], Muhammad Ismail [1,b], Haris Pervaiz [c], Rachad Atat [e], I. Safak Bayram [*,f], Qiang Ni [d]

[a] James Watt School of Engineering, University of Glasgow, Glasgow
[b] Dept. of Computer Science, Tennessee Technological University, Cookeville, TN USA
[c] School of computer science and electronic engineering University of Essex, Colchester, UK
[d] School of Computing and Communications, Lancaster University, UK
[e] Rachad Atat is with the Dept. of ECE, Texas A&M University at Qatar
[f] Dept. of Electronic and Electrical Engineering, University of Strathclyde, Glasgow, UK

A B S T R A C T

Real-time monitoring in smart grids requires efficient handling of massive amount of data. Fog cloud nodes can be strategically located within the smart grid to: pull readings from smart meters, implement local processing and control, and make all data available to the smart grid control center with minimum overall latency. Unlike existing studies in literature, we propose a novel Fog node allocation strategy that is tightly coupled with the power grid structure, and hence, accounts for the spatial distribution of data traffic sources (e.g., smart meters) within the power grid. Furthermore, the allocation strategy considers the diverse latency requirements of fixed scheduling and event driven data services within the power grid. The proposed allocation strategy first implements an unsupervised machine learning approach to determine initial number and locations of Fog nodes that can serve the data traffic with minimum overall latency. Then, a reinforcement-based mechanism is applied to minimize the required number of Fog nodes, and hence capital cost, through efficient mapping between Fog nodes and smart meters while still complying with the latency requirements. Our simulation studies demonstrate that a 50% reduction in required number of Fog nodes can be achieved while minimizing overall latency when the proposed allocation strategy is adopted.

1. Introduction

1.1. Motivation

To enable the advanced services offered by future smart grids, there is a need to strengthen the interplay between power systems and communication networks. Specifically, wider adoption of disruptive technologies such as distributed energy generators, distributed storage units, electric vehicles, and demand response will be possible thanks to state-of-the-art real-time monitoring and notification systems that incorporate phasor measurement units and smart meters along with the existing supervisory control and data acquisition (SCADA) systems [1]. These devices will rely on integrated communication networks to transmit various grid-related data including: (i) demand-side related data such as energy consumption levels, (ii) operational related data such as power quality status and optimal control strategies, and (iii) energy market data for peer-to-peer or larger scale market participation. For instance, in a field study conducted in Austin, TX with nearly one thousand homes equipped with solar panels, electric vehicles, and smart meters, one billion daily data is created and handled with cloud service [2]. Obtaining high resolution data is particularly critical for electricity service providers as this data enables fast detection of grid failures and faults as well as an accurate forecast of supply and demand. Inefficient handling of such tasks lead to immediate financial losses. Therefore, significant amount of data, with tight latency requirements, need to be exchanged among different components within the grid in a timely manner.

Traditional power grids adopt a centralized communication infrastructure in which remote terminal units transmit data to a centralized controller. However, as the power system operations become more data-centric, there is a need for a more effective networking paradigm for efficient data management [3]. In this context, cloud-based infrastructure offers a scalable, flexible, and dynamic solution to handle high

* Corresponding author.
E-mail addresses: muhammadali.jamshed@glasgow.ac.uk (M.A. Jamshed), mismail@tntech.edu (M. Ismail), haris.pervaiz@essex.ac.uk (H. Pervaiz), rachad.atat@qatar.tamu.edu (R. Atat), safak.bayram@strath.ac.uk (I.S. Bayram), q.ni@lancaster.ac.uk (Q. Ni).

[1] This publication was made possible by NPRP12S-0221-190127 from the Qatar National Research Fund (a member of Qatar Foundation). The statements made herein are solely the responsibility of the authors.

https://doi.org/10.1016/j.prime.2023.100144
Received 19 November 2022; Received in revised form 22 January 2023; Accepted 11 March 2023
Available online 18 March 2023

Nomenclature

QoS	quality of service
IoT	Internet of things
FN	fog node
FNs	fog nodes
ED	event driven
FS	fixed scheduling
ML	Machine learning
RL	Reinforcement learning
GERoNIMO	Generalized EMF Research using Novel Methods
APs	access points

is the problem of collecting and analyzing data. Traditional methods for gathering data in smart grids can be expensive in terms of computation and communication. To overcome these challenges, recent efforts have been focused on utilizing fog computing in combination with smart grids [4]. As illustrated in Fig. 1, a hierarchical architecture can be adopted in the smart grid using Fog cloud nodes for data collection and control services [5,6]. In this model, the power grid is divided into regions (clusters) and a Fog node is assigned to each region. Data collected from smart meters is transmitted to the corresponding Fog node where local data processing and control take place. Further, data is forwarded to a control center that is typically hosted in the core cloud for global co-ordination. Such a cloud-based networking solution was shown to result in a significant cost reduction, $14 million, compared to traditional networking solutions [5].

While selecting an appropriate networking technology is imperative

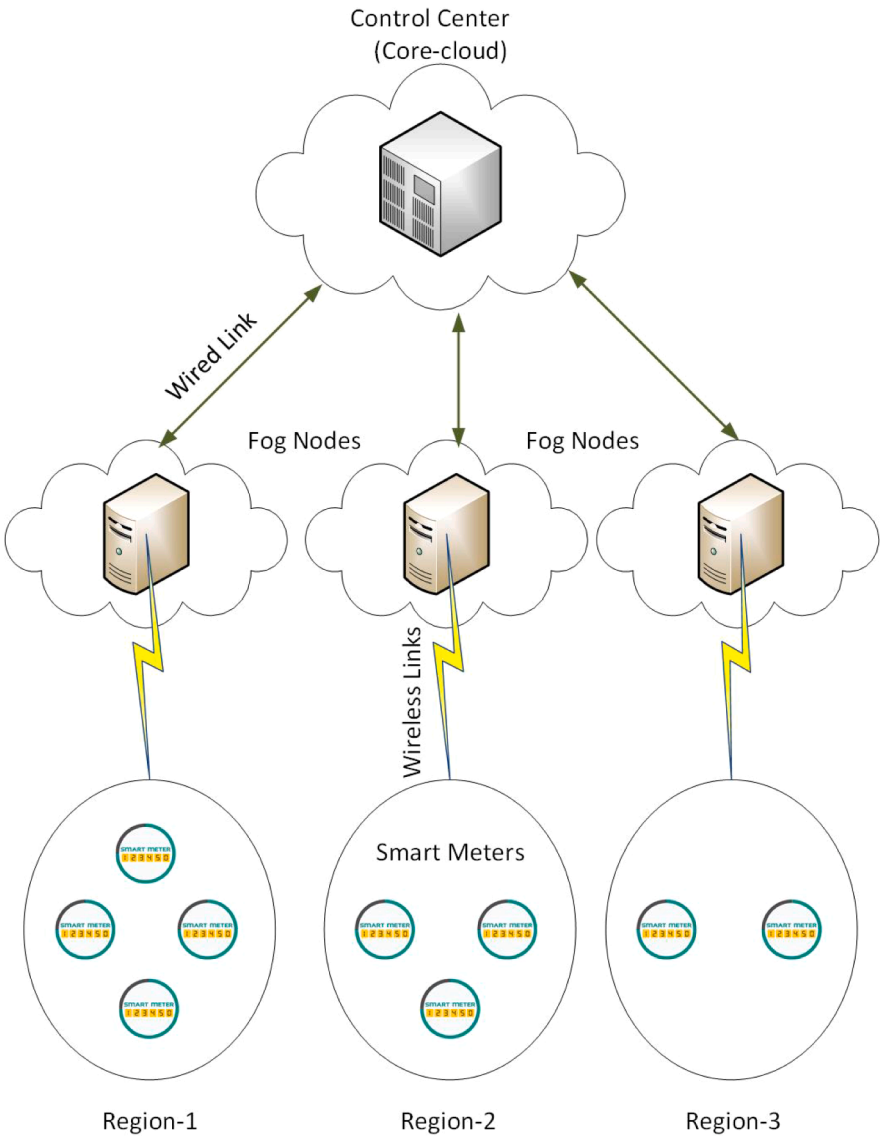

Fig. 1. Hierarchical cloud architecture in smart grid.

volumes of data traffic with minimum latency, thanks to the concept of edge and Fog cloud nodes. The use of fog and edge computing can effectively handle tasks such as managing data for large IoT systems. One major issue that needs to be addressed in the next generation of smart grid IoT systems, which consist of a large number of smart devices, for successful operation of smart grids, optimal design of such networks is equally important. In the context of cloud-based smart grids, careful planning of Fog node placement is critical to provide a reliable, high-performing, and cost-effective data management. To minimize the overall communication latency, which is vital for emergency services

Table 1
Taxonomy of Recent Literature

Ref.	Algorithm	Application	Latency consideration
[14]	Heuristic	Electric vehicles	Yes
[20]	Heuristic	Electric vehicles	No
[21]	Heuristic	Energy systems	Yes
[22]	Cooperative scheduling	Smart grid	Yes
[15]	Machine learning	Smart grid	Yes

within the power grid, an optimal allocation strategy is needed to determine the optimal locations of Fog nodes.

1.2. Related work and limitations

Cloud-based smart grid services have been the subject of several studies [3,5–11]. In [3], a hierarchical cloud-based architecture is proposed and its application for direct load control in smart grid is discussed. In [5], cloud computing is adopted to offer security-as-a-service for advanced metering infrastructure (AMI). In [6], an open-source platform is proposed for data management and sharing within the power grid based on cloud computing. In [7], a cloud-based demand response architecture and a set of distributed algorithms are presented to enable secure, scalable, and reliable demand response programs. In [8], a cloud-based load forecasting framework is proposed to minimize energy consumption and carbon emissions in micro-grids by reducing both message overhead and energy consumption. In [9], a cloud-based electric vehicle demand management is proposed for public charging stations. In [10], a decentralized Fog cloud architecture is proposed for energy management of electric vehicles. In [12], the authors proposed a resource allocation based strategy to study the impact of pricing on service delay. In [13], the authors propose a low complex heuristic solution to optimize the delay in Fog enabled cloud based systems. In [11], a cloud computing based hierarchical electric vehicle charging management model is proposed. Two levels of cloud nodes are considered to satisfy different delay requirements of customers seeking to receive service in highway exits and parking lots. Similarly in [14] and using a multi-level could computing mechanism, a cost efficient charging system is proposed for electric vehicles.

Allocation of measurement and communication devices in smart grids has been studied in a handful of studies [1,15–17]. In [1], placement of data aggregation units in a smart grid network is formulated as a mixed integer linear programming problem that minimizes network congestion. In [15], an allocation problem is formulated as basic cost minimization that aims to find the location and number of data aggregation units needed to provide connectivity between customers and grid operators. In [16], an allocation problem of data aggregation units with wired connectivity is formulated and solved by linear programming relaxation. This model is further expanded in [17] to include wireless connectivity. In [18], the software defined networking approach is introduced to reduce the cost of aggregation points in large smart grid systems. In [19], a neural network is embedded at the edge of the smart grid network to increase the utilization of the resources as well as the throughput of the system. A brief comparison of some of the recent literature is also provided in Table 1.

Overall, existing studies on allocation of aggregators/Fog nodes do not accurately account for the topological features of the power grid. The existing allocation strategies do not take into consideration the power grid structure and spatial distribution of smart meters within the power grid while specifying the optimal Fog node locations. Since the smart meters located in the power grid are the main sources of data traffic, it is critical to account for their spatial distribution while formulating the Fog node allocation problem, which helps in minimizing the latency of both link access and end-to-end connection. Further, it is important to note that the density of the data sources (e.g., smart meters, etc.) does not follow an even distribution among different regions as highlighted in [23]. Hence, the generated data traffic at different clusters represents inhomogeneous spatial distribution, which further impacts the optimal number and locations of Fog nodes.

1.3. Our contributions

The objective of this work is to address the limitations of existing research by proposing an optimal allocation strategy of Fog nodes that is tightly coupled with the power grid structure and spatial distribution of smart meters. The detailed contributions of this work can be summarized as follows:

- We propose a two-step optimal allocation strategy of Fog nodes that is well integrated with the power grid topology and the spatial distribution of data traffic within the grid. The proposed strategy aims to minimize the end-to-end latency within the network using the minimum number of Fog nodes in order to reduce the associated capital investment costs.
- We adopt an unsupervised machine learning approach based on K-means to specify the candidate number and locations of Fog nodes that are needed to serve the data traffic generated from the smart meters across the grid.
- Based on the candidate locations of Fog nodes, we then propose a reinforcement learning-based strategy (multi-armed bandit (MAB)) in order to optimally map the smart meters and Fog nodes in a way that associates the smart meters to the minimum number of Fog nodes, and hence, reduce the number of required Fog nodes to serve the data traffic while minimizing the end-to-end latency.
- We evaluate the performance of the proposed allocation strategy using Monte Carlo simulations. Our results demonstrate that the proposed reinforcement learning-based strategy leads to a reduction in the number of Fog nodes by 50% while satisfying the end-to-end latency with minimum computational complexity.

1.4. Organization

The rest of the paper is organized as follows: In Section II, the details of the proposed system model are provided. In Section III, the proposed fog node allocation strategy is explained. In Section IV, the performance of the proposed methodology is validated using simulation results and comparing with benchmark scheme. Finally, we present the conclusion in Section V.

2. System model

In this section, we present the system model that consists of the power grid structure along with the location of smart meters, wireless communication channel, and queuing process.

2.1. Power grid structure

In order to properly design a network that ensures acceptable communication coverage within the power grid, geographical locations of buses, and hence, smart meters, is required. Unfortunately, this information is not available using the standard IEEE bus test systems. Furthermore, obtaining geographical locations of actual power grids is pretty hard and usually comes with strict non-disclosure agreement due to national security measures, which limits sharing the results with the research community. To overcome this limitation, a generative power grid model is proposed in [23] based on stochastic geometry, which presents accurate spatial approximations to real power grids. Comparison results of the stochastic geometry-based power grid model and actual power grids revealed a similarity score of more than 90%. Hence, we will adopt the stochastic geometry-based power grid model of [23] to establish a power grid structure that reflects a realistic spatial distribution of bus nodes, and hence, smart meters.

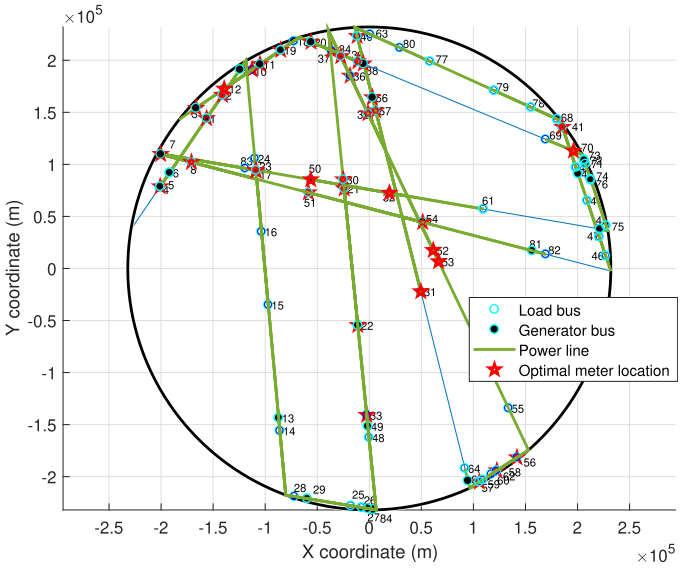

Fig. 2. An example of a realization of the stochastic geometry-based power grid model for a transmission system with 84 buses, 31 of which are generators. Solid lines represent power lines and light lines represent roads. The optimal locations of meters are marked with a star symbol according to [23].

For completeness, we present a brief summary to construct the power grid model of [23] following the steps below:

(1) The process starts by generating lines (roads) in a disk of radius R, representing a region $\mathscr{A}$, such as a city. For this, the Poisson line space is used, where each line ℓ_l is defined by an angle direction $0 \leq \theta_l < 2\pi$ and by length $0 < p_l \leq R$. The number of lines intersecting $\mathscr{A}$ is $2\pi\lambda_l R$, where λ_l is the density of the Poisson line process (PLP) Φ_l.

(2) Buses are added on each Poisson line $\ell_l \in \Phi_l$ following the one-dimensional (1D) homogeneous Poisson point process (HPPP), $\Phi_{\mathrm{p},l}$, with density $\lambda_{\mathrm{p},l}$. Summing over all the lines in $\mathscr{A}$, the buses constitute an HPPP Φ_{B} with density $\lambda_{\mathrm{B}} = \sum_{l=1}^{2\pi\lambda_l R} \lambda_{\mathrm{B},l}$. The total number of buses, B, in the network is expressed as $B = \sum_{l=1}^{2\pi\lambda_l R} \lambda_{\mathrm{B},l}|\ell_l|$, with $|\ell_l| = 2R\sin(\cos^{-1}(p_l/R))$.

(3) Buses are connected together via power lines based on their physical paths by selecting one of the potential near-geodesic routes [24] and by using the shifted sum of exponential distributions of the degree of buses [25].

(4) Disconnected buses are linked based on the shortest pathways between them to decrease power losses and assure power supply to all loads. Finally, load capacities are assigned to buses by matching the real values and the developed ones based on their corresponding probabilities [26].

2.2. Locations of smart meters

To define the locations of smart meters, which defines the spatial distribution of data sources within the grid, we follow the optimal placement strategy presented in [23]. The optimal locations of meters are defined to absorb a certain amount of uncertainty in the power grid. The continuous and stable operation of power grids depend on efficient state estimation, load monitoring, and fault detection. Deployment of metering and monitoring devices will extract real-time information which to keep the power grid stable. Therefore, the optimal locations of meters are defined to absorb a certain amount of uncertainty in the power grid. The uncertainty comes from insufficient and inaccurate real-time data measurements, as well as the unpredictable time-varying loads and renewable energy generation. The amount of uncertainty, u_{s_b}, absorbed by smart meter s_b located at bus b, is defined as a fraction of the b^{th} bus degree to the degree of all of its children buses[2] that are not assigned a smart meter within a cluster polygon, $\mathscr{P}(o,R_c)$, centered at o and with diameter R_c. Thus,

$$u_{s_b} = \frac{\deg(b)}{\sum_{i\in\{\{k_b^{\mathscr{P}}\}\setminus\{\mathscr{B}\},b\}}\deg(i)}, \tag{1}$$

where $\deg(b)$ is the degree of bus b, $\{k_b^{\mathscr{P}}\}$ is the set of the nearest neighbors to bus b within the cluster polygon $\mathscr{P}$, and $\mathscr{B}$ is the set of buses with already allocated smart meters.

Then, the influential buses where smart meters need to be installed are identified. To obtain a solution for the optimal locations of smart meters, the following steps are taken:

- Graph trees are constructed from the power grid model according to Algorithms 1 and 2 in [23].
- Identifying central nodes in a network is critical to designing a network that is resilient against faults or attacks. However, identifying which nodes are vital in a network is a nontrivial task. In literature, a number of different centrality metrics exist (e.g. Eigenvector, Diffusion, Authority and Hub) for different networks (e.g. communications, transportation, power) [27]. In this article, Katz Centrality is adopted to improve the grid's state estimation. Katz Centrality uses a new status measure by considering the number of direct connections to a node and the statuses of nodes connected to the node. Therefore, it is well-suited for power networks as this centrality metric identifies buses with the highest number of connections with other buses. The reason of selecting this metric is that the closer a nonabsorbable bus (i.e., without a smart meter) is to an observable bus, the better the grid status can be inferred.
- The amount of uncertainty absorbed by buses is then calculated according to (1).
- Finally, with a predetermined budget to be spent for smart metering deployment, optimal locations of smart meters can be determined to achieve a 90% uncertainty absorption using a constrained finite-horizon Markov decision process (MDP) algorithm [23].

Fig. 2 shows a sample realization of the stochastic geometry-based power grid model with 84 buses, 31 of which act as generators while the rest act as loads. The optimal locations of metering equipment that achieve 90% uncertainty absorption are highlighted with a star symbol. In total, 38 smart meters are allocated to achieve the target observability. As shown in Fig. 2, the X-Y coordinates of buses and smart meters are indicated, which is necessary for optimal allocation of Fog nodes to ensure communication coverage. For simplicity of notation, from now on, smart meters will be referred to as s instead of s_b, $s \in \mathscr{S} = \{1,2,\cdots,S\}$.

2.3. Communication channel model

Each smart meter s uploads its data to the assigned Fog node using a 4G LTE wireless link [28,29]. The network bandwidth W is divided into K sub-carriers. Orthogonal frequency division multiplexing (OFDM) is adopted, where smart meter s is allocated sub-carrier k at time slot t. The allocated sub-carrier to one smart meter cannot be shared by another smart meter. On the other hand, the Fog nodes are directly connected to the core cloud (control center), using a high speed wired optical link as

[2] Each bus is considered to be a parent bus, to which all physical connections with immediate and non-immediate neighboring buses are identified. These neighbors are referred to as children buses.

shown in Fig. 1.

The transmitted signal from smart meter s to Fog node g, at distance d_{sg}, suffers from a path loss that is given by [30]

$$\mathrm{PL}(d_{sg}) = \alpha(d_{sg}) \times \mathrm{PL}_{\mathrm{LoS}}(d_{sg}) + (1 - \alpha(d_{sg})) \times \mathrm{PL}_{\mathrm{NLoS}}(d_{sg}), \tag{2}$$

where $\alpha(d_{sg})$, $\mathrm{PL}_{\mathrm{LoS}}(d_{sg})$, and $\mathrm{PL}_{\mathrm{NLoS}}(d_{sg})$ denote the line-of-sight (LoS) probability, LoS path loss, and non-LoS (NLoS) path loss, respectively. The LoS probability is given by

$$\alpha(d_{sg}) = \max\left\{1, \exp^{\frac{(-d_{sg}+10)}{200}}\right\}, \tag{3}$$

and the LoS and NLoS path losses are given by

$$\mathrm{PL}_{\mathrm{LoS}}(d_{sg}) = 24.8 + 20\log_{10}(F) + 24.2\log_{10}(d_{sg}), \tag{4}$$

$$\mathrm{PL}_{\mathrm{NLoS}}(d_{sg}) = 20\log_{10}(F) + 42.8\log_{10}(d_{sg}) - 3.3, \tag{5}$$

where F denotes the carrier frequency.

In addition to the path loss, the transmitted signal is affected by small scale fading, which follows a Nakagami-m distribution. Hence, the signal amplitude fading ξ follows the probability density function (PDF) given by

$$f_{\Xi}(\xi) = \frac{2m^m \xi^{2m-1}}{\Gamma(m)\Omega^m} \exp^{-\left(\frac{m}{\Omega}\right)\xi^2}, \tag{6}$$

where $\Omega = \mathbb{E}[\xi^2] > 0$ with $\mathbb{E}[\cdot]$ denotes the expectation operator, the Nakagami parameter $m = (\mathbb{E}^2[\xi^2])/(x^2 - \mathbb{E}[\xi^2])^2 \geq 0.5$, and $\Gamma(\cdot)$ is the gamma function.

The power grid within region $\mathscr{A}$ is covered by a single wireless macro-cell that adopts the OFDM technology, and hence there is no interference among the transmitted signals of different smart meters. Thus, the signal-to-noise-ratio (SNR) for smart meter s communicating with Fog node g over sub-carrier k, γ_{sgk}, is given by

$$\gamma_{sgk} = \frac{P_{sgk} \times h_{sgk}}{\sigma^2}, \tag{7}$$

where P_{sgk}, h_{sgk}, and σ^2 respectively denote the transmitted signal power, channel gain, and noise power. For planning purposes, Monte Carlo simulation is adopted where h_{sgk} channels are sampled using the PDF of Nakagami-m fading $f_{\Xi}(\xi)$ in (6) for K sub-carriers allocated to S smart meters over T iterations. The path loss impact is also considered according to (2) based on the distance d_{sg} for each smart meter s and Fog node g.

2.4. Data traffic and queuing model at fog nodes

Data traffic due to smart meters is classified into fixed-scheduling and event-driven traffic [31]. The fixed scheduling traffic is transmitted periodically between the smart meters and the Fog node for normal operations. On the other hand, the event-driven traffic is generated in response to a critical demand-response condition. Two separate queues are assumed per Fog node to properly handle each traffic class. Fixed-scheduling data packets are transmitted from smart meter s following a deterministic batch arrival process with rate Λ_s^F, while event-driven data packets are transmitted from smart meter s following a Poisson random process with rate Λ_s^E. The overall arrival rates of data packets at Fog node g for fixed-scheduling and event driven queues are given by $\Lambda_g^F = \sum_{s \in \mathscr{S}_g} \Lambda_s^F$ and $\Lambda_g^E = \sum_{s \in \mathscr{S}_g} \Lambda_s^E$, respectively, where $\mathscr{S}_g$ denotes the set of smart meters under the jurisdiction of Fog node g. A single server is considered per Fog node and a deterministic service rate μ_g is employed. Since event-driven traffic reflects an emergency condition, it is processed with higher priority at the Fog node than the fixed-scheduling traffic. The traffic intensity at Fog node g can be calculated as $\rho_g^{\mathrm{F/E}} = \Lambda_g^{\mathrm{F/E}}/\mu_g$, for fixed-scheduling and event-driven queues.

The priority of each transmitted packet from a smart meter follows the rules of preemptive-resume priority [32]. Hence, an absolute priority is given to the event driven packets over the fixed scheduling packets. Each smart meter transmits the data packets with a preemptive-resume priority, i.e., once the event driven packets are generated, the transmission of fixed scheduling packets is paused. Furthermore, the service of a fixed scheduling packet is interrupted when an event driven packet arrives at the Fog node. Once there are no more event driven data packets to be served at the Fog node, the server resumes the service of the fixed scheduling packets from the point where it was interrupted. Hence, fixed scheduling packets have spent more time in the queue with mean waiting time [32]

$$W_g^F = \frac{1/\mu_g}{(1-\rho^E) \times (1-\rho^E-\rho^F)} - \frac{1}{\mu_g}. \tag{8}$$

On the other hand, the mean waiting time for the event-driven packets is given by [32]

$$W_g^E = \frac{\rho_g^E}{2\mu_g \times \left(1-\rho_g^E\right)}. \tag{9}$$

2.5. End-to-End delay model

The end-to-end latency considers both: (1) data transmission latency from the smart meters to the Fog nodes, which reflects the time delay for a successful reception of data packet at the Fog node. This term is affected by the wireless channel condition and the relative distance between the smart meter and the Fog node, and (2) queuing latency that reflects the delay of data processing at the Fog nodes before handling the data packet (for further forwarding to the control center or for taking a control action upon the information in the data packet). This term is affected by the arrival rate of data packets and the processing capabilities of the Fog node.

The end-to-end average delay Δ_{sg} is defined as the time taken by a data packet to be transmitted from smart meter s and processed by Fog node g on average. This is given by

$$\Delta_{sg}^{\mathrm{F/E}} = \Delta_{sg}^{\mathrm{TX}} + \Delta_{sg}^{\mathrm{Q(E/F)}}, \tag{10}$$

where $\Delta_{sg}^{\mathrm{TX}}$ denotes the average transmission delay for successful reception of the packet and Δ_{sg}^{Q} represents the average queuing delay. The transmission delay assumes negligible propagation delay and accounts mainly for packet re-transmissions. Hence, it depends on the relationship between the SNR γ_{sgk} and a decoding threshold κ. Assuming a maximum of 3 transmissions allowed per packet [33], the transmission delay can be expressed as

$$\begin{cases} \Delta_{sg}^{\mathrm{TX}} = 0, & \text{if } \gamma_{sgk}^{(1)} > \kappa \\ \tau, & \text{if } \gamma_{sgk}^{(1)} < \kappa \\ 2\tau, & \text{if } \gamma_{sgk}^{(2)} < \kappa, \end{cases} \tag{11}$$

where $\gamma_{sgk}^{(1)}$ and $\gamma_{sgk}^{(2)}$ denote the SNR values at the first and second transmissions, respectively, and τ is a unit delay. The expression in (11) is averaged using Monte Carlo simulations based on the PDF in (6). On the other hand, the average queuing delay can be described by [32]

$$\Delta_{sg}^{\mathrm{Q(F/E)}} = W_g^{\mathrm{F/E}} + \frac{1}{\mu_g}. \tag{12}$$

INPUT: $\mathbb{S}$ and $\tilde{G}$
Step 1: Finding Optimal Number of Fog Nodes
for $G = 1, \ldots, \tilde{G}$ **do**
    Use K-means to form Clusters of $\mathbb{S}$
    Find the mean Silhouette φ_G using (16) - (18)
end for
Step 2: Optimal Candidate Number of Fog Nodes
Find the value of G that corresponds to $\max_{G} \varphi_G$
Step 3: Optimal Candidate Locations of Fog Nodes
Use K-means to place G Fog nodes and specify their locations as centroids of the clusters
OUTPUT: G and $\boldsymbol{Y}$

Algorithm 1. Specification of Candidate Number and Locations of Fog Nodes

INPUT: $\mathcal{S}$, $\mathbb{S}$, $\mathcal{G}$, T, Υ, and Δ
for $t = 1, \ldots, T$ **do**
    if $t == 1$ **then**
        Step 1: Initial Assignment
        for $s = 1, \ldots, S$ **do**
            while *s is unassigned* **do**
                Assign s to g that presents the maximum channel gain $\Upsilon(s, :)$ while satisfying $\Delta_{sg}^{\mathrm{F/E}} \leq \epsilon_{\mathrm{F/E}}$.
            end while
        end for
    else
        Step 2: UCB-MAB Assignment
        for $s = 1, \ldots, S$ **do**
            Allocate smart meter s to Fog node g following the policy in (21)
        end for
    end if
end for
Step 3: Update G **and** $\boldsymbol{Y}$
Discard any unutilized Fog node g and update $\mathcal{G}$ and $\boldsymbol{Y}$ accordingly
OUTPUT: G, $\boldsymbol{Y}$, $\boldsymbol{X}$

Algorithm 2. MAB-based Fog Allocation Strategy

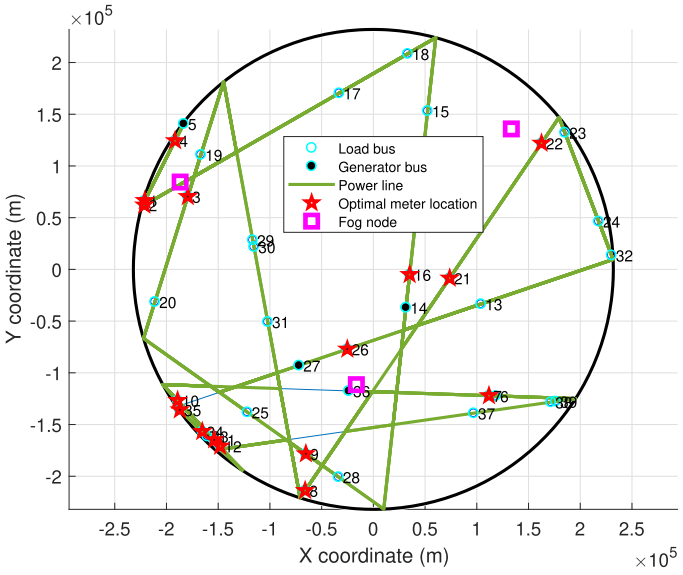

Fig. 3. Stochastic geometry-based power grid model for a transmission system with 39 buses and 16 smart meter. Three Fog nodes are allocated according to our proposed strategy.

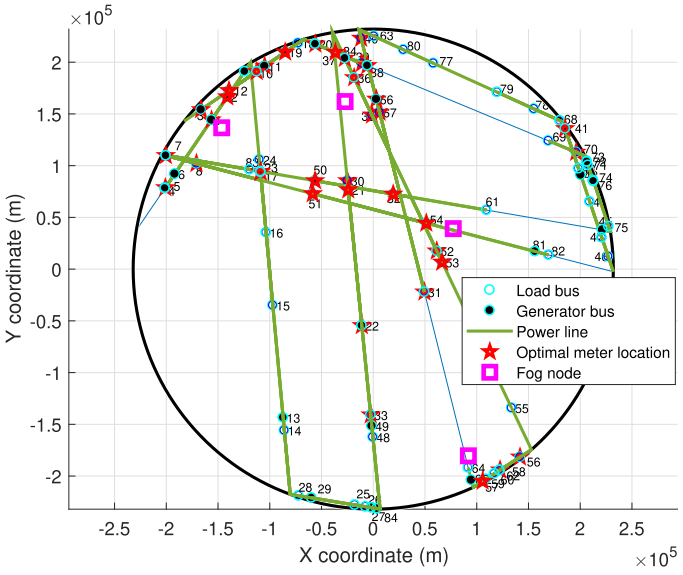

Fig. 4. Stochastic geometry-based power grid model for a transmission system with 84 buses and 38 smart meter. Four Fog nodes are allocated according to our proposed strategy.

3. Efficient allocation strategy of fog nodes

Our objective is to allocate the minimum number of Fog cloud nodes that can serve the data traffic generated by the smart meters while ensuring minimum end-to-end latency. In turn, this would minimize the capital investment cost to install and maintain such Fog nodes. This can be expressed as follows

$$\min_{G,\boldsymbol{X},\boldsymbol{Y}} \sum_{g=1}^{G} \sum_{b=1}^{B} y_{gb} \left[\sum_{s=1}^{S} x_{sg} \left(\Delta_{sg}^{F} + \Delta_{sg}^{E} \right) \right], \tag{13}$$

Subject to:

$$\Delta_{sg}^{\mathrm{F/E}} \leq \epsilon_{\mathrm{F/E}}, \ \forall s, \ \forall g \tag{14}$$

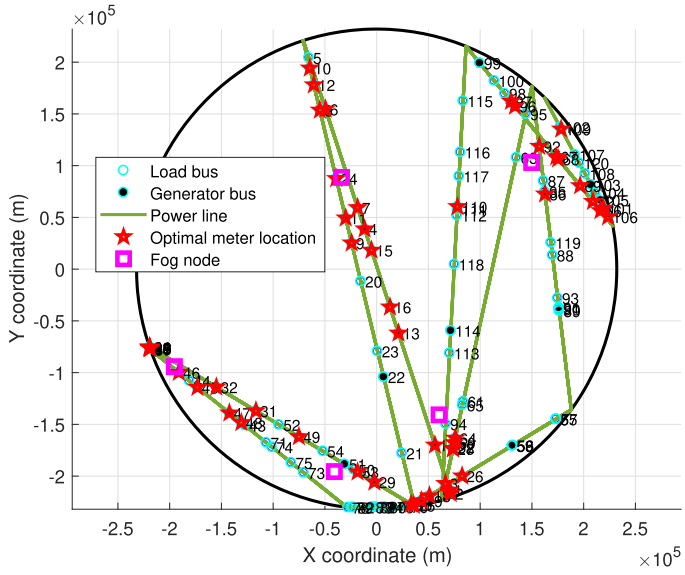

Fig. 5. Stochastic geometry-based power grid model for a transmission system with 120 buses and 54 smart meter. Five Fog nodes are allocated according to our proposed strategy.

$$\sum_{b=1}^{B} y_{gb} \leq 1 \ \forall g, \quad \sum_{s=1}^{S} x_{sg} \leq 1, \ \forall s \tag{15}$$

$$\epsilon_{\mathrm{F/E}} \geq 0, \quad G \in \mathbb{Z}^{+}, \quad \boldsymbol{X}, \boldsymbol{Y} \in \{0, 1\}. \tag{16}$$

The decision variables in (13) are: (a) the number of allocated Fog nodes G, which is a positive integer $\in \mathbb{Z}^{+}$, (b) the location of Fog node g, y_{gb}, which is a binary indicating whether Fog node g is allocated at the location of bus b, and (c) the assignment of smart meter s to Fog node g, x_{sg}, which is also binary. Constraint (14) ensures that the average delay for fixed scheduling and event-driven packets satisfy a respective target threshold $\epsilon_{\mathrm{F/E}}$, which presents a non-negative and small value. Constraint (15) allocates a given Fog node to one and only one location b, and assigns a smart meter to one and only one Fog node. The allocation of the Fog nodes in (13) accounts for the transmission delay, which is function of the distance (i.e., relative location) and channel conditions between smart meter s and Fog node g, as described by y_{gb} and x_{sg}. Furthermore, the allocation accounts for the queuing delay, which is a function of the number of assigned Fog nodes and the assignment of smart meters to Fog nodes, as described by G and x_{sg}. All aforementioned decision variables are impacted by the spatial distribution of the smart meters and their relevant data traffic.

The allocation in (13) represents combinatorial optimization, which incurs expensive computational complexity, especially in large power grids [34]. Hence, in the following subsections, we present an efficient allocation strategy that presents low computational complexity. The proposed solution aims at decoupling the decision variables by dividing (13) into two sub-problems. The first sub-problem aims to specify a candidate number G and locations $\boldsymbol{Y}$ of Fog nodes to be installed in the system. The second sub-problem aims to find an optimal assignment of smart meters to Fog nodes $\boldsymbol{X}$ such that the minimum number of Fog nodes are installed while satisfying the target latency requirements.

3.1. Candidate number and locations of fog nodes

In order to specify the candidate number and locations of Fog nodes, we resort to an unsupervised learning technique, namely, K-means clustering. The rationale behind choosing this approach is that by clustering the smart meters and allocating a Fog node to serve each

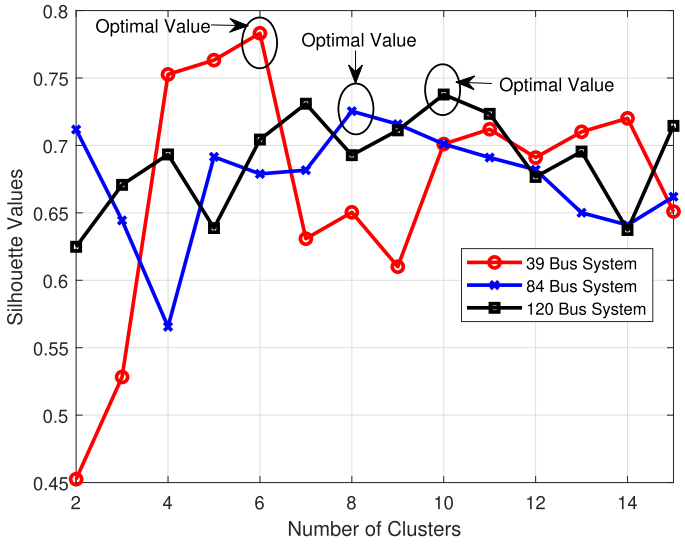

Fig. 6. Determining the candidate number of Fog nodes.

Table 2
Average delay experienced by the fixed scheduling (FS) and event-driven (ED) packets under Algorithm 2

Fog node Index	Average Delay FS (sec.)	Average Delay ED (sec.)
	39 Bus System	
2	1.4021	0.0294
3	2.2433	0.047
6	0.8412	0.0176
	84 Bus System	
1	3.9258	0.0822
2	2.5237	0.0529
5	0.8412	0.0176
6	3.3649	0.0705
	120 Bus System	
1	3.9258	0.0822
2	2.2433	0.047
3	3.0845	0.0646
7	2.8041	0.0587
9	3.0845	0.0646

Table 3
Average delay experienced by the fixed scheduling (FS) and event-driven (ED) packets under Exhaustive search

Fog node Index	Average Delay FS (sec.)	Average Delay ED (sec.)
	39 Bus System	
2	3.9258	0.0822
3	0.5608	0.0118
	84 Bus System	
1	3.9258	0.0822
2	3.9258	0.0822
6	3.3649	0.0588
	120 Bus System	
1	3.9258	0.0822
2	3.9258	0.0822
3	3.9258	0.0822
7	3.3649	0.0705

cluster, we are minimizing the transmission delay, which constitute one part of the end-to-end delay. It should be highlighted that such an approach does not provide any guarantee that the minimum number of Fog nodes are allocated or that the queuing (and overall end-to-end) delay is satisfied. Hence, the first sub-problem merely serves as an initialization step for the second sub-problem.

In this sub-problem, we aim to cluster the S smart meters, whose geographical locations are known, into $1 \leq G \ll S$ clusters. A Fog node is allocated at the centroid of each cluster g in order to serve the smart meters within this cluster. Let $\mathbb{S}$ denote the geographical location of the smart meters within the power grid and $\mathcal{G}$ represents the set of clusters. The K-means algorithm clusters $\mathbb{S}$ into G clusters that minimize a cost function $J(G) = \sum_G \| \mathbb{S}_g - \Sigma_g \|^2$, where Σ_g denotes the mean geographical location (centroid) of cluster g. Hence, a fundamental step is to specify the number of clusters G. A plethora of techniques are available in the literature to find an optimal value of G, however, there is no agreed-upon solution [35]. In this paper, we have adopted a well-known clustering validation technique, namely, the Silhouette method [36].

The Silhouette method is based on Silhouette value φ_{sg} that measures the similarity of a data point (in $\mathbb{S}$) between assigned cluster g and other clusters (in $\mathcal{G} \backslash g$). These values assume a range $[-1, 1]$, where a high value indicates that the data point is well matched to its cluster and a low value indicates that the number of clusters is insufficient or exceeded the limit. Let V_{sg} quantifies the suitability of assigning smart meter s to cluster g based on the similarity between location of smart meter s and other meters assigned to cluster g. Hence, we have

$$V_{sg} = \frac{1}{|g| - 1} \sum_{s' \in g, s' \neq s} d_{s,s'}, \tag{17}$$

where $|g|$ denotes the number of smart meters in g and $d_{s,s'}$ represents the distance between two smart meters s and s' in cluster g. The average dissimilarity between smart meter s in g and smart meters assigned to other cluster $g' \in \mathcal{G} \backslash g$ is

$$U_{sg} = \min_{g' \neq g} \frac{1}{|g'|} \sum_{s' \in g', g' \in \mathcal{G} \backslash g} d_{s,s'}. \tag{18}$$

Based on V_{sg} and U_{sg}, the Silhouette value φ_{sg} can be calculated according to the following relationship

$$\begin{cases} \varphi_{sg} = 1 - \dfrac{V_{sg}}{U_{sg}}, & \text{if } V_{sg} < U_{sg} \\ 0, & \text{if } V_{sg} = U_{sg} \\ \dfrac{U_{sg}}{V_{sg}} - 1, & \text{if } V_{sg} > U_{sg}. \end{cases} \tag{19}$$

The mean Silhouette value φ_G can then be found by calculating the mean Silhouette values for all data points in $\mathbb{S}$, i.e.,

$$\varphi_G = \frac{1}{|\mathbb{S}|}\sum_{\mathbb{S}} \varphi_{sg}. \tag{20}$$

Algorithm 1 summarizes the steps taken in order to determine the optimal number and locations of Fog nodes based on K-means clustering. The input to Algorithm 1 is the geographical location of smart meters $\mathbb{S}$ and an initial guess for the number of clusters $\widetilde{G}$. The process starts by running the K-means clustering algorithm for a different number of clusters G. Each time, the mean Silhouette value φ_G is recorded. The optimal number of Fog nodes G is the one that presents the maximum mean Silhouette value. The φ_G is calculated for each G (as shown in Line 5 of Algorithm 1) then the optimal G is found as the one corresponding to the largest φ_G (as shown in Line 8 of Algorithm 1). Finally, Algorithm 1 runs the K-means clustering using the specified optimal number of Fog nodes G in order to specify their locations $\boldsymbol{Y}$ as the centroids of the clusters in $\mathscr{G} = \{1, 2, \cdots, G\}$.

3.2. Optimal allocation strategy

The candidate allocation strategy outlined in the previous subsection does not guarantee that the minimum number of Fog nodes being installed. Furthermore, such a candidate solution does not ensure that the assignment of smart meters to the Fog nodes result in a traffic load distribution that satisfies the queuing latency requirement. As discussed in the previous subsection, the goal so far has been to find an initial allocation strategy that we may refine later to maximize the utilization efficiency of the Fog nodes, by associating the smart meters to the minimum number of Fog nodes while satisfying the end-to-end latency requirements. By doing so, some of the planned Fog nodes to be allocated will not be utilized, and hence, we can revise the initial allocation strategy and discard the allocation of such unutilized Fog nodes. In this subsection, we resort to a reinforcement learning strategy, namely MAB, in order to carry out this smart meter-Fog node association, i.e., finding $\boldsymbol{X}$ in (13), and revise the initial allocation strategy, i.e., specifying final values for G and $\boldsymbol{Y}$. Owing to the binary nature of the problem and the associated computational complexity, a heuristic optimization technique may be used. On the other hand, a MAB-based solution results in a near-optimal allocation strategy with reduced complexity.

The main idea behind reinforcement learning is to learn from the environment using an agent that selects the best action based on experiences to yield the maximum reward. In this context, the agents/players are the S smart meters, and the machines/states of the environment are the G Fog nodes. Hence, in the MAB-based assignment strategy, each smart meter $s \in \mathscr{S}$ plays G Fog nodes for multiple times and selects a Fog node $g \in \mathscr{G}$, which maximizes the reward Ψ_{sg} that reflects the satisfaction of the latency requirements. Let $\Psi_{sg}(t) = 1$ if smart meter s selects a Fog node g that satisfies the end-to-end latency requirements, at iteration t, and at the same time Fog node g is serving as many smart meters as possible. Otherwise, $\Psi_{sg}(t) = 0$. This reward definition associates the smart meters to the minimum number of Fog nodes while at the same time satisfying the latency requirements. At each iteration, this reward is random as it depends on the wireless channel conditions and the queuing process at the Fog nodes. The main target of the MAB is to find an assignment strategy that maximizes the average reward over T iterations. Specifying the optimal assignment requires that smart meter s tries all G Fog nodes to estimate the expected reward, a process that is referred to as the learning phase. During this phase, smart meter s learns to select Fog node g that maximizes the long term average reward. This is done by choosing the best Fog node g that is known so far, which is know as exploitation, while also exploring other Fog node options $\mathscr{G} \backslash g$ in hope of finding a better solution, which is known as exploration.

In literature, there exists a plethora of methods to solve this exploitation versus exploration trade-off. In this paper, we adopt the upper confidence bound (UCB) approach as it offers an optimal solution with minimal storage and processing requirements [37]. Hence, the assignment action taken by smart meter $s \in \mathscr{S}$ during iteration t, $\pi_s(t)$, is the one that maximizes the following function

$$\pi_s(t) = \underset{g \in \mathscr{G}}{\operatorname{argmax}} \left[\overline{\Psi}_{sg}(t) + c \times \sqrt{\frac{\ln(t)}{N_{sg}(t)}} \right], \tag{21}$$

where $\overline{\Psi}_{sg}(t)$ is the average reward of an action $\pi_s(t) = g$ that is taken by smart meter s at iteration t, given by

$$\overline{\Psi}_{sg}(t) = \frac{1}{N_{sg}(t)} \sum_{\tau=1}^{t} \Psi_{sg}(\tau) \mathbb{1}_{(\pi_s(\tau)=g)}, \tag{22}$$

where $N_{sg}(t)$ in (21) and (22) denotes the number of times smart meter s selects Fog node g until iteration t, c in (21) is the exploration coefficient. The term inside the square root of (21) is referred to as the confidence interval of average reward $\overline{\Psi}_{sg}(t)$. Hence, the assignment in (21) is based on the past experience, which converges over time to the optimal policy.

Algorithm 2 summarizes the steps taken to carry out the smart meter-Fog node assignment strategy to find the optimal $\boldsymbol{X}$ and to update the optimal values of G and $\boldsymbol{Y}$. The input to the algorithm is the number of Fog nodes G, their IDs $\mathscr{G}$, and their respective locations $\boldsymbol{Y}$ as obtained from Algorithm 1. Further, the set of smart meters $\mathscr{S}$ and their respective locations are used as inputs. Moreover, sample channel gain matrix Υ is generated by sampling the PDF expression in (6). The rows and columns of Υ are the smart meters and Fog nodes. Algorithm 2 is run for several times ($\sim 10^3$ iterations) for different Υ samples and the average policy is then recorded. The algorithm also takes the end-to-end delay matrix Δ as described by (10) - (12) and number of iterations T as input. At the first iteration, the algorithm finds an initial assignment by mapping smart meter s to Fog node g that presents the highest channel gain and satisfies the end-to-end delay requirement. Over the next iterations, the assignment strategy is carried out based on the UCB in (21). Upon completing all iterations, the number of Fog nodes G and their locations $\boldsymbol{Y}$ are updated such that the unutilized Fog nodes from Algorithm 1 are discarded.

3.3. Computational complexity

The proposed allocation strategy consists of two phases, namely on K-means and MAB. The worst case computational complexity of K-means algorithm is $\mathscr{O}(S^2)$. Whereas, the computational complexity of the Silhouette method used within the K-means is $\mathscr{O}(S^2)$. Algorithm 1 is iterated over G, and generally we have $G << \mathbb{S}$. Hence, the worst case computational complexity of Algorithm 1 is $\mathscr{O}(2S\log(S))$. Furthermore, the computational complexity of Algorithm 2 that is based on the MAB UCB scheme is $\mathscr{O}(\log(S))$. On the other hand, adopting an exhaustive search to directly solve the allocation in (13) presents a worst case complexity of $\mathscr{O}(2^{S/2})$.

4. Performance evaluation

This section presents performance evaluation results of the proposed allocation strategy versus benchmark solutions.

4.1. Benchmark and parameter setup

We compare the performance of the proposed two-step allocation strategy to two benchmark solutions. The first allocates the Fog nodes using only Algorithm 1. In this case, upon specifying G and $\boldsymbol{Y}$ based on Algorithm 1, each smart meter s is assigned to the Fog node g at the centroid of its cluster. The second benchmark adopts a more complex exhaustive search method, which jointly finds optimal value of G and $\boldsymbol{Y}$, as well as the optimal assignment for each smart meter. It is noted that, in exhaustive search method the location of each g fog node is found using K-means.

The following simulation parameters are used in our investigations

unless otherwise stated. The transmit power of all smart meters are set to 23 dBm. The end-to-end delay thresholds are set to $\epsilon_F = 4$ seconds and $\epsilon_E = 1$ second. The exploration coefficient $c = 1.5$. The packet arrival rates are $\Lambda_s^F = 0.026$ and $\Lambda_s^E = 0.0023$, while $\mu_g = 1/3$. The value of Λ_s^E is calculated based on the number of outages in the power grid. We have used the statistics provided by Eaton [38] and as a case study we consider California, who has experienced 4300 outages in 2018. An upper bound of 3 re-transmissions is set for successful packet delivery, otherwise the packet is lost. The total capacity of the network is defined as the sum of the total available capacity at each Fog node, i.e., $G \times \epsilon_F$ for fixed scheduling packets and $G \times \epsilon_E$ for event driven packets, respectively.

We conduct a set of three experiments to cover different sizes of the power grid, and hence, explore the scalability of our proposed solution. Hence, we consider the following simulation setups:

- Small power grid size of 39 buses. Based on [23], the power grid has 16 smart meters, as shown in Fig. 3.
- Medium power grid size of 84 buses. Based on [23], the power grid has 38 smart meters, as shown in Fig. 4.
- Large power grid size of 120 buses. Based on [23], the power grid has 54 smart meters, as shown in Fig. 5.

4.2. Simulation results

Fig. 6 shows the mean Silhouette value φ_G versus the number of clusters $\widetilde{G}$. Based on Algorithm 1, Fig. 6 suggests that the candidate number of Fog nodes are 6, 8, and 10 to support the small, medium, and large power grid sizes, respectively. The output of Algorithm 1 is then fed to Algorithm 2 to determine the optimal smart meter-Fog node assignment, and hence, further reduces the number of required Fog nodes. The results of Fog allocation based on Algorithm 2 for the small, medium, and large power grid sizes are shown in Figs 3 - 5, respectively. As shown in figures, only 3, 4, and 5 Fog nodes are required to satisfy the target latency requirements. These represent a 50% reduction in the number of candidate allocations as recommended by Algorithm 1.

Table 2 summarizes the average delay experienced by data packets when Algorithm 2 is adopted. As can be seen in Table 2, Algorithm 2 reduces the number of required Fog nodes for the small size power grid from 6 as suggested by Algorithm 1 to only 3 Fog nodes. Similarly, for medium and large power grid sizes, the number of Fog nodes are reduced to 4 and 5, respectively. Table 2 confirms that such a reduction in number of Fog nodes does not come at the expense of sacrificing any end-to-end delay requirements. Table 3 summarizes the average delay experienced by data packets when exhaustive search is adopted instead of Algorithm 2. As shown in Table 3, exhaustive search results in the allocation of 2, 3, and 4 Fog nodes. While exhaustive search provides an optimal solution, the near-optimal solution provided by Algorithm 2 is merely less than the optimal solution by 16%, 12%, and 10% for the small, medium, and large size power grids. Two remarks can be made here. First, the optimality gap decreases as the size of the grid increases. Second, exhaustive search presents exponential complexity, unlike our proposed algorithm that offers a much reduced (logarithmic) complexity, as discussed in Section III.C. Hence, the proposed algorithm offers a better scalability than an exhaustive search approach.

5. Conclusion

This paper proposes a two-step allocation strategy of Fog nodes in cloud-based smart grids. The allocation strategy captures the spatial distribution of smart meters and data traffic within the power grid, and aims to install the minimum number of Fog nodes that can satisfy target end-to-end delay and at the same time provide a low complexity and a scalable solution. The first step specifies candidate number and locations of Fog nodes based on K-means clustering, which are further refined in the second step based on MAB. The proposed strategy can reduce the number of installed Fog nodes by 50%, while satisfying the target end-to-end latency. In our future work, we plan on investigating real-time routing strategies based on reinforcement learning to guarantee on-time delivery of fixed scheduling and event-driven data packets among the Fog nodes and the core-cloud node.

Declaration of Competing Interest

The authors declare that they have no known competing financial interests or personal relationships that could have appeared to influence the work reported in this paper.

Data availability

No data was used for the research described in the article.

References

[1] T. Zhen, T. Elgindy, S.M.S. Alam, B.-M. Hodge, C.D. Laird, Optimal placement of data concentrators for expansion of the smart grid communications network, IET Smart. Grid. 2 (4) (2019) 537–548.
[2] P. Street, Pecan Street online database, 2016, (https://www.pecanstreet.org/about/).
[3] F. Luo, J. Zhao, Z.Y. Dong, Y. Chen, Y. Xu, X. Zhang, K.P. Wong, Cloud-based information infrastructure for next-generation power grid: conception, architecture, and applications, IEEE Trans. Smart Grid 7 (4) (2016) 1896–1912.
[4] A. Saleem, A. Khan, S.U.R. Malik, H. Pervaiz, H. Malik, M. Alam, A. Jindal, Fesda: fog-enabled secure data aggregation in smart grid iot network, IEEE IoT J. 7 (7) (2019) 6132–6142.
[5] M. Hasan, H. Mouftah, Cloud-centric collaborative security service placement for advanced metering infrastructures, IEEE Trans. Smart Grid 10 (2) (2019) 1339–1348.
[6] D. Anderson, T. Gkountouvas, M. Meng, K. Birman, A. Bose, C. Hauser, E. Litvinov, X. Luo, Q. Zhang, Gridcloud: infrastructure for cloud-based wide area monitoring of bulk electric power grids, IEEE Trans. Smart Grid 10 (2) (2018) 2170–2179.
[7] S. Bera, T. Ojha, S. Misra, M.S. Obaidat, Cloud-based optimal energy forecasting for enabling green smart grid communication. 2015 IEEE Global Communications Conference (GLOBECOM), IEEE, 2015, pp. 1–6.
[8] S. Bera, T. Ojha, S. Misra, M.S. Obaidat, Cloud-based optimal energy forecasting for enabling green smart grid communication. 2015 IEEE Global Communications Conference (GLOBECOM), IEEE, 2015, pp. 1–6.
[9] D.A. Chekired, L. Khoukhi, Smart grid solution for charging and discharging services based on cloud computing scheduling, IEEE Trans. Ind. Inf. 13 (6) (2017) 3312–3321.
[10] D.A. Chekired, L. Khoukhi, H.T. Mouftah, Queuing model for evs energy management: load balancing algorithms based on decentralized fog architecture. 2018 IEEE International Conference on Communications (ICC), IEEE, 2018, pp. 1–6.
[11] C. Kong, B.P. Rimal, B.P. Bhattarai, M. Devetsikiotis, Cloud-based charging management of electric vehicles in a network of charging stations. 2018 IEEE International Conference on Communications (ICC), IEEE, 2018, pp. 1–6.
[12] S.C. Misra, A. Mondal, Fogprime: dynamic pricing-based strategic resource management in fog networks, IEEE Trans. Veh. Technol. 70 (8) (2021) 8227–8236.
[13] J. Du, L. Zhao, X. Chu, F.R. Yu, J. Feng, I. Chih-Lin, Enabling low-latency applications in LTE-a based mixed fog/cloud computing systems, IEEE Trans. Veh. Technol. 68 (2) (2018) 1757–1771.
[14] C. Kong, B.P. Rimal, M. Reisslein, M. Maier, I.S. Bayram, M. Devetsikiotis, Cloud-based charging management of heterogeneous electric vehicles in a network of charging stations: Price incentive vs. capacity expansion, IEEE Trans. Serv. Comput. (2020).
[15] M. Tavasoli, M.H. Yaghmaee, A.H. Mohajerzadeh, Optimal placement of data aggregators in smart grid on hybrid wireless and wired communication. 2016 IEEE Smart Energy Grid Engineering (SEGE), IEEE, 2016, pp. 332–336.
[16] X. Huang, S. Wang, Aggregation points planning in smart grid communication system, IEEE Commun. Lett. 19 (8) (2015) 1315–1318.
[17] X. Huang, S. Wang, C. Wang, Aggregation points planning for smart grid communications: wired and wireless cases. 2015 IEEE Global Communications Conference (GLOBECOM), 2015, pp. 1–6.
[18] S. Wang, X. Huang, Aggregation points planning for software-defined network based smart grid communications. IEEE INFOCOM 2016-The 35th Annual IEEE International Conference on Computer Communications, IEEE, 2016, pp. 1–9.
[19] Q. Li, Y. Deng, W. Sun, W. Li, Communication and computation resource allocation and offloading for edge intelligence enabled fault detection system in smart grid. 2020 IEEE International Conference on Communications, Control, and Computing Technologies for Smart Grids (SmartGridComm), IEEE, 2020, pp. 1–7.
[20] S. Gao, R. Dai, C. Li, W. Cao, Cloud-edge collaborative distributed optimal bidding strategy for large-scale EVs in electricity markets. 2022 IEEE Vehicle Power and Propulsion Conference (VPPC), 2022, pp. 1–6, https://doi.org/10.1109/VPPC55846.2022.10003343.

[21] X. Zhu, J. Yang, X. Zhan, Y. Sun, Y. Zhang, Cloud-edge collaborative distributed optimal dispatching strategy for an electric-gas integrated energy system considering carbon emission reductions, Int. J. Electric. Power Energy Syst. 143 (2022) 108458.
[22] S. Chouikhi, M. Essegir, L. Meerghem-Boulahia, Energy consumption scheduling as a fog computing service in smart grid, IEEE Trans. Serv. Comput. (2022).
[23] R. Atat, M. Ismail, M.F. Shaaban, E. Serpedin, T. Overbye, Stochastic geometry-based model for dynamic allocation of metering equipment in spatio-temporal expanding power grids, IEEE Trans. Smart Grid 11 (3) (2020) 2080–2091.
[24] W. Kendall, Networks and poisson line patterns: fluctuation asymptotics, Oberwolfach Rep. 5 (2008) 2670–2672.
[25] D. Deka, S. Vishwanath, R. Baldick, Analytical models for power networks: the case of the western U.S. and ERCOT grids, IEEE Trans. Smart Grid 8 (6) (2017) 2794–2802, https://doi.org/10.1109/TSG.2016.2540439.
[26] S.H. Elyas, Z. Wang, R.J. Thomas, On the statistical settings of generation and load in a synthetic grid modeling, The 10th Bulk Power Syst. Dyn. Control Symp. (IREP 2017) (2017).
[27] Z. Wan, Y. Mahajan, B.W. Kang, T.J. Moore, J.-H. Cho, A survey on centrality metrics and their network resilience analysis, IEEE Access 9 (2021) 104773–104819, https://doi.org/10.1109/ACCESS.2021.3094196.
[28] M. Erol-Kantarci, H.T. Mouftah, Energy-efficient information and communication infrastructures in the smart grid: a survey on interactions and open issues, IEEE Commun. Surv. Tutor. 17 (1) (2014) 179–197.
[29] S. Bu, F.R. Yu, Y. Cai, X.P. Liu, When the smart grid meets energy-efficient communications: green wireless cellular networks powered by the smart grid, IEEE Trans. Wirel. Commun. 11 (8) (2012) 3014–3024.
[30] J. Wu, S. Rangan, H. Zhang, Green communications: theoretical fundamentals, algorithms, and applications, CRC press, 2016.
[31] O. Al-Khatib, W. Hardjawana, B. Vucetic, Traffic modeling and optimization in public and private wireless access networks for smart grids, IEEE Trans. Smart Grid 5 (4) (2014) 1949–1960.
[32] I. Adan, J. Resing, Queueing Theory, Eindhoven University of Technology. Department of Mathematics and Computing Q, 2001.
[33] K. Ghoumid, D. Ar-Reyouchi, S. Rattal, R. Yahiaoui, O. Elmazria, et al., An accelerated end-to-end probing protocol for narrowband iot medical devices, IEEE Access 9 (2021) 34131–34141.
[34] P. Toth, Optimization engineering techniques for the exact solution of NP-hard combinatorial optimization problems, Eur. J. Oper. Res. 125 (2) (2000) 222–238.
[35] R. Tibshirani, G. Walther, T. Hastie, Estimating the number of clusters in a data set via the gap statistic, J. R. Stat. Soc.: Ser. B (Stat. Methodol.) 63 (2) (2001) 411–423.
[36] S. Aranganayagi, K. Thangavel, Clustering categorical data using silhouette coefficient as a relocating measure. International Conference on Computational Intelligence and Multimedia Applications (ICCIMA 2007) volume 2, IEEE, 2007, pp. 13–17.
[37] R.S. Sutton, A.G. Barto, Reinforcement Learning: An Introduction, second, The MIT Press, 2018.
[38] B.T. Eaton, United States Annual Report 2018. Technical Report, Technical Report, 2018. Available online: http://powerquality. eaton. com..., 2018.

Muhammad Ali Jamshed (Member, IEEE) received the B.Sc. degree in electrical engineering from COMSATS University, Islamabad, Pakistan, in 2013, the M.Sc. degree in wireless communications from the Institute of Space Technology, Islamabad, in 2016, and the Ph.D. degree from the University of Surrey, Guildford, U.K., in 2021. He is endorsed by the Royal Academy of Engineering under exceptional talent category. He served briefly as a Wireless Research Engineer with BriteYellow Ltd., U.K., and then moved to the James Watt School of Engineering, University of Glasgow, as a Postdoctoral Research Assistant. He has contributed to a patent (under review) and authored/coauthored two book chapters and more than 28 technical papers in leading journals and peer-reviewed conferences. His main research interests include EMF exposure reduction, low SAR antennas for mobile handsets, machine learning for wireless communication, backscatter communication, and wireless sensor networks. He was nominated for the Departmental Prize for Excellence in Research by the University of Surrey in 2019. He is also serving as a Reviewer for IEEE Wireless Communications Letters. Moreover, he served as a Reviewer, a TPC Member, and the Session Chair for many well-known conferences, such as ICC, WCNC, VTC, and GLOBECOM, and other scientific workshops.

Muhammad Ismail received the B.Sc. (Hons.) and M.Sc. degrees in electrical engineering from Ain Shams University, Egypt, in 2007 and 2009, respectively, and the Ph.D. degree in electrical and computer engineering from the University of Waterloo, Canada, in 2013. He is an assistant professor with the Computer Science Department, Tennessee Tech. University, USA. He received the best paper awards from IEEE IS'20, IEEE TCGCN in IEEE ICC'19, IEEE Globecom'14, IEEE ICC'14, Green'16, SGRE'15. He is an associate editor with IEEE IoTJ and IEEE TGCN

Haris Pervaiz (Member, IEEE) received the M.Sc. degree in information security from the Royal Holloway University of London, Egham, U.K., in 2005, and the Ph.D. degree from the School of Computing and Communication, Lancaster University, Lancaster, U.K., in 2016. He was a Research Fellow with the 5G Innovation Centre, University of Surrey, Guildford, U.K., from 2017 to 2018, and an EPSRC Doctoral Prize Fellow with the School of Computing and Communication, Lancaster University, from 2016 to 2017, where he is currently working as a Lecturer with the InfoLab21. He has been actively involved in projects, such as CROWN, CogGREEN, TWEETHER, the Energy Proportional EnodeB for LTE-Advanced and Beyond and the DARE Project, and an ESPRC funded project. His current research interests include green heterogeneous wireless communications and networking, 5G and beyond, millimeter wave communication, and energy and spectral efficiency. He is also an Associate Editor of IEEE Access, IET Quantum Communication, IET Networks, Transactions on Emerging Telecommunications Technologies (Wiley), and Internet Technology Letters (Wiley).

Rachad Atat (Member, IEEE) received the Ph.D. (Hons.) degree in electrical engineering from the University of Kansas (KU), Lawrence, KS, USA, in 2017.,He is currently a Postdoctoral Research Associate with Texas A&M University at Qatar (TAMUQ), Doha, Qatar, working on cybersecurity strategies for smart grids. His current research interests include smart grids, cybersecurity, and Internet of Things.,Dr. Atat was the recipient of the 2016 IEEE GLOBECOM Best Paper Award, the KU Engineering Fellowship Award, and the National Science Foundation and TAMUQ Travel Grant Awards.

I. Safak Bayram (Senior Member, IEEE) received the B.S. degree in electrical and electronics engineering from Dokuz Eylul University, Izmir, Turkey, in 2007, the M.S. degree in telecommunications from the University of Pittsburgh, in 2010, and the Ph.D. degree in electrical and computer engineering from North Carolina State University, in 2013. From January 2014 to December 2014, he worked as a Postdoctoral Research Scientist at Texas A&M University at Qatar. From 2015 to 2018, he was an Assistant Professor with the College of Science and Engineering and a Staff Scientist with the Qatar Environment and Energy Research Institute and Hamad Bin Khalifa University. Since 2019, he has been a Lecturer or an Assistant Professor (Chancellor's Fellow) with the University of Strathclyde, Glasgow, U.K. He received the Best Paper Award at the Third IEEE International Conference on Smart Grid Communications and the First IEEE Workshop on Renewable Energy and Smart Grid, in March 2015.

Qiang Ni (Senior Member, IEEE) received the B.Sc., M.Sc., and Ph.D. degrees in engineering from the Huazhong University of Science and Technology, China. He led the Intelligent Wireless Communication Networking Group, Brunel University London, U.K. He is currently a Professor and the Head of the Communication Systems Group, InfoLab21, School of Computing and Communications, Lancaster University, Lancaster, U.K. His main research interests lie in the areas of wireless communications and networking, including green communications, cognitive radio systems, 5G, the Internet-of-Things, and vehicular networks. He was an IEEE 802.11 Wireless Standard Working Group Voting Member and a Contributor to the IEEE Wireless Standards